Microbially Induced Corrosion of Carbon Steel and Stainless Steel in Alkaline Ground Water – Composition and Metabolic Functionality of Biofilm – 14391

Pauliina Rajala, Leena Carpén, Mikko Vepsäläinen, Malin Bomberg, Mari Raulio
VTT Technical Research Centre of Finland, Kemistintie 3/Tietotie 2, 02044 VTT, Finland

ABSTRACT

Low and intermediate level nuclear waste composed mainly of carbon and stainless steel produced during operation, maintenance and decommissioning of nuclear power plants is disposed of in underground repository, which will be exposed to groundwater. The corrosive effect of groundwater and microbes naturally occurring in groundwater on carbon and stainless steel is assumed to be decreased, when pH of the groundwater has increased due to its contact with the concrete of the repository silos. Nevertheless, after one-year exposure to the repository environment, including the alkaline effect of concrete, the formation of biofilm on the steel surfaces was not completely inhibited, but mainly slowed down. According to weight loss determinations the presence of concrete clearly diminished the corrosion rates of carbon steel at least in the early stages of biofilm formation. No corrosion or biofilm were detected on the surfaces of stainless steel. Our results demonstrate that especially methylotrophic bacteria of the α-proteobacterial clade play a main role in the initial biofilm formation under repository conditions.

INTRODUCTION

Low and intermediate level nuclear waste is produced during operation, maintenance and decommissioning of nuclear power plants. In Finland, low and intermediate level waste is packed into concrete silos and disposed of in the underground repository excavated into the bedrock 60–100 meters below sea level. The metallic waste consists mostly of carbon steel and stainless steel.

It is known that the groundwater at this depth contains up to 10^5 microbes mL^{-1} with considerable vast diversity [1]. Microorganisms may greatly contribute to corrosion of carbon steel and stainless steel. They are able to accelerate several types of corrosion, such as general corrosion, and localized corrosion, e.g. pitting and stress corrosion cracking, as well as degradation of concrete. However, the effect of microbial activity on the corrosion of decommissioning waste and the release of radioactive nuclides is still unclear and needs to be studied further.

In oxygen free water the corrosion of carbon steel is low, unless water is very acidic or there is microbial activity in the environment. At disposal sites, the concrete generates a high pH environment, which significantly decreases the corrosion rate of carbon steel. Over the course of time pH starts to decrease again, e.g. due to the carbonization of concrete. As a consequence of lower pH and accelerated corrosion rate of the metallic waste, radioactive nuclides may be released into groundwater and carried to the neighboring area of the repository. The effect of microbial activity on the corrosion of decommissioning waste and the release of radioactive nuclides needs to be studied further.

The results of this simulation study can be used to evaluate the risks of the microbially induced corrosion of metallic materials in the underground repository.

METHODS

Experimental setup

A study simulating the repository conditions was set up in Olkiluoto in October 2011 in the cave constructed as repository for disposal of low and intermediated radioactive waste at a depth of 100 m below sea level. The experiment consisted of 43 L glass mesocosms, containing crushed concrete and untreated, anaerobic groundwater from the disposal site to simulate the repository conditions. The concrete was similar to that used in the bedrock silos for low and intermediate level waste from Olkiluoto Nuclear Power Plant. Carbon steel (AISI/SAE 1005) and stainless steel (EN 1.4301, AISI304) coupons were surface sterilized in 70% ethanol and rinsed in the groundwater immediately before they were placed in sterile glass holders in the N_2 flushed glass mesocosms. Anaerobic groundwater was lead directly from the drill hole through factory clean polyamide tube to the mesocosms.

In order to evaluate microbially induced corrosion as well as corrosion caused by other than microbial mechanisms, both biotic and abiotic mesocosms were prepared. Abiotic mesocosms were prepared by injecting 20 mL methylisothiazolinone (9.5% V/V, ProClin® 950, Sigma-Aldrich) and 12 mL glutaraldehyde (25% V/V, VWR International), anaerobically into the mesocosms using sterile plastic syringes. The mesocosms were sealed with ground glass caps and the joints were sealed with silicon grease and tightened with steel wire in order to prevent oxygen leakage into the mesocosms.

To mimic the slow flow of groundwater and dissolved substances possibly affecting the corrosion and microbial growth, half of the water volume of the mesocosms was replaced after 6 months with fresh anaerobic groundwater. After the change of water, biocides were added to the abiotic mesocosms as described above.

After 1 year of incubation, water samples were collected into acid washed, sterile N_2 flushed glass bottles equipped with butyl rubber stoppers and open top screw caps for microbiological and chemical water analyses. In addition, pH, O_2 content, conductivity and redox-potential were measured from the removed water on site. These measurements were conducted also in the beginning of the experiment and during the water change after 6 months. The steel coupons for microbiological studies were removed from the mesocosms under constant N_2 flow and packed in sterile and DNAase free plastic tubes and placed directly on dry ice. The steel coupons for corrosion studies were quickly removed from the mesocosms under N_2 flow and immediately immersed in 96% ethanol, air dried and placed in glass desiccators for transport to the laboratory. In the laboratory, each steel coupon was imaged using a digital camera.

Materials

Low alloy carbon steel (AISI/SAE 1005/UNS G10050) from cold-rolled thin sheet and stainless steel (AISI 304, UNS S30400) from wrought plate were used as materials for test coupons. The surfaces of the materials were as received and the coupon size was 27 mm x 71 mm. Prior to the incubation the length, width and thickness of the coupons were measured. All steel coupons were cleaned with deionized water and ethanol and air-dried. The coupons for weight loss measurements were weighed with the accuracy of 0.1 mg, after which they were sterilized in 70% ethanol.

Microbiological analyses

To analyze the planktonic microbial community, the microbial biomass of 250 mL subsamples was collected anaerobically from water in the mesocosms on the 0.22 µm Sterivex® -filtration units (Millipore, MA, USA) at the end of experiment and the samples were stored at -80°C until DNA extraction. The biofilm was extracted from the surface of the steel coupons by bead beating coupons in 10 mL sterile phosphate buffered saline (PBS) and Tween®20 (Merck, Germany) (1 µL Tween®20 1 mL^{-1} PBS) for 20 minutes at 150 rpm agitation and followed by ultra-sonication for 3 min. The biomass released from the steel coupons was subsequently collected on 0.22 µm Sterivex™ -filtration units (Millipore, MA, USA) for subsequent DNA extraction. The filters of the water samples and biofilm were prepared for DNA extraction by first breaking the filter units with sterile pliers and cutting out the filter membranes. The DNA was subsequently extracted using the PowerWater® DNA Isolation kit (MoBio Laboratories, Inc., CA, USA) in accordance with the manufacturer's protocol and the DNA was eluted in 50 µL elution buffer supplied by the manufacturer. Negative DNA extraction controls were included in the DNA extractions.

As a proxy for bacterial biomass, quantitative PCR (qPCR) was used to determine the amount of 16S rRNA gene copies in each sample. The amount of sulfate reducing microbes was determined on base of copies of β-subunit of dissimilatory sulfite reductase (*dsr*B) gene. The presence of methanogenic archaea was studied using qPCR targeting the α-subunit of methyl coenzyme-M reductase (*mcr*A) gene. qPCR was performed in 10 µL reaction volumes using the LightCycler® 480 qPCR machine and LightCycler® 480 Software 1.5.0 (Roche Applied Science, Germany). The reaction mixture contained 1 µL template, standard dilution or water, 1 × KAPA SYBR® FAST Universal qPCR Master Mix (KAPA Biosystems, MA, USA), 2.5 µM of both forward and reverse primer (P1 and P2 for 16S rRNA gene, DSRp2060F and DSR4R for *dsr*B gene, ME1 and ME3 for *mcr*A gene) and nuclease free water [2, 3, 4, 5]. A ten-fold dilution series of plasmids containing the bacterial 16S rRNA gene, *dsr*B gene or *mcr*A gene ranging from 10^1 to 10^9 copies per reaction was used to estimate the concentration of corresponding gene copies in the samples and no template controls. The PCR program consisted of an initial 15 min incubation at 95°C, followed by 45 cycles of denaturation at 95°C for 10 s, annealing at 55°C for 35 s and extension 72°C for 30 s, and with final extension at 72°C for 3 min. Sample fluorescence was measured at the end of each elongation phase. Subsequently, a melting curve was recorded, to test the specificity of the qPCR, with a program consisting of 10 s of denaturation at 95°C, 1 min of annealing at 65°C, and a melting and continuous measuring step rising gradually (20°C s^{-1}) to 95°C.

For pyrosequencing the bacterial 16S rRNA gene fragments were amplified with primers 8F and P2 equipped with adapter and barcode sequences at their 5' as described by Bomberg *et al* [6, 7]. The amplification was performed in 50 µL reaction volumes, containing 2 µL template, 1 × Maxima HotStart buffer (Fermentas), dNTP 0.2 mM each (final concentration) (Fermentas), $MgCl_2$ 4 mM (final concentration) (Fermentas), 0.2 µM (final concentration) of both forward- and reverse primers (Eurogentec, Seraing, Belgium), 1.5 U Maxima HotStart polymerase (Fermentas) and nuclease free H_2O (Sigma, MO, USA). The amplification in all PCR reactions was carried out on a thermal PCR cycler (Mastercycler® gradient, Eppendorf, Hamburg, Germany) using the following conditions: 95°C initial denaturation for 4 min, followed by 40 cycles of 94°C for 1 min, 55°C for 1 min and 72°C for 1 min, with final extension step at 72°C for 15 min. Amplicons were purified using the NucleoSpin® kit (Macherey-Nagel, Germany)

according to the manufacturer's protocol. Amplicon libraries were sequenced by Macrogen Inc. (Seoul, Korea). The sequences obtained from the amplification libraries were analyzed with the Mothur software [8]. Due to the high number of similar sequences obtained, the sequences were grouped into operational taxonomic units (OTUs). Each OTU consisted of 16S rRNA sequences sharing over 97% of the nucleic acid sequence. One representative sequence was chosen from each sample for each OTU. To perform phylogenetic analyses the sequences were imported into the Geneious Pro Software package (version 5.5.6, Biomatters Inc., Auckland, NZ) [9]. Relevant reference sequences and sequences of type species were included in the phylogenetic analyses. The sequences were aligned using MUSCLE in Geneious Pro. Maximum likelihood analysis was performed on the nucleic acid sequence alignments using PhyML [10] with the Jukes-Cantor substitution model [11]. Bootstrap support for the nodes was calculated on 1000 random repeats.

Corrosion analyses

Corrosion was evaluated by weight loss of the coupons and type of the corrosion was verified under a stereomicroscope. Carbon steel and stainless steel coupons were weighed, cleaned with a brush and pickled according to the ASTM standard G 1-90 [12]. To determine the mass loss of the base metal during the removal of the corrosion products, a replicate uncorroded control specimen was cleaned by the same procedure as the test specimens. The mass losses were determined and the average corrosion rates (µm a^{-1}) were calculated according to the ASTM standard G 1-90 [12].

The corrosion products of selected coupons were analyzed with an energy-dispersive x-ray spectrometry (EDS) coupled to scanning electron microscopy (SEM). The surface analysis and visual examination of deposits was performed by applying field-emission scanning electron microscopy (FE-SEM). Samples for FE-SEM were prepared as previously described by Carpén *et al*. [13].

RESULTS

The chemical composition of groundwater in the beginning of the experiment was analyzed along the water from mesocosms in the end of the one-year experiment to be able to observe the changes due to concrete addition and possible differences between the biotic and abiotic environment (TABLE I).

Groundwater in the beginning of the experiment had pH 7.9, O_2 0.5 mg L^{-1}, γ 3.1 mS cm^{-1}, redox potential 120 mV vs SHE, alkalinity 4.9 mmol L^{-1}, Cl^- 454 mg L^{-1}, SO_4^{2-} 124 mg L^{-1}. Half of the water volume was changed after 6 months of immersion from the water taken from the same drill hole. The groundwater composition differed slightly from the conditions in the beginning of the experiment; the pH was a little higher, 8.5, redox potential lower, 51 mV vs SHE but chloride, sulphate, conductivity as well as oxygen were at same level as in the beginning of the experiment (436 mg L^{-1}, 112 mg L^{-1}, 3.3 mS cm^{-1}, 0.7 mg L^{-1}, respectively).

pH increased from 7.9 in the incoming groundwater to 11-12 due to the presence of concrete (TABLE I). The rise of pH contributes to the solubility and precipitation of chemical components in water. During the one-year incubation period the concentration of total sulfur, sulfate and total organic carbon (TOC) decreased in the biotic mesocosms whereas the concentration of nitrite increased (TABLE I). In the abiotic mesocosms the amount of TOC increased (TABLE I). This is

most probably due to the biocides added to these mesocosms. The concentration of dissolved aluminum increased considerably, most likely due to the effect of concrete, and the concentration of dissolved manganese decreased during the incubation period compared to the groundwater at the beginning of the experiment (TABLE I). Free carbon dioxide could predispose steel to corrosion but after one-year the CO_2 is consumed entirely.

TABLE I. The chemical composition of ground water at the beginning of the experiment and the composition of water from mesocosms after one-year. Arrows are indicating the change in chemical composition, - indicates no change.

		Ground water	AISI/SAE 1005 biotic		AISI/SAE 1005 abiotic		EN 1.4301 biotic		EN 1.4301 abiotic	
pH		7.9	12	↑	11	↑	12	↑	11	↑
Alk	mmol L^{-1}	4.9	6.77	↑	5.3	↑	6.19	↑	6.03	↑
TOC	mg L^{-1}	14	11	↓	62	↑	6.3	↓	62	↑
CO_2	mg L^{-1}	12	<1	↓	<1	↓	<1	↓	<1	↓
SO_4	mg L^{-1}	124	90	↓	94	↓	94	↓	95	↓
PO_4	mg L^{-1}	0.3	<0.02	↓	<0.02	↓	<0.02	↓	<0.02	↓
NO_2	mg L^{-1}	<0.04	0.1	↑	<0.04	-	0.1	↑	<0.04	-
NO_3	mg L^{-1}	<2	<2	-	<2	-	<2	-	<2	-
NH_4	mg L^{-1}	0.14	0.25	↑	0.27	↑	0.23	↑	0.27	↑
Na	mg L^{-1}	343	346	-	343	-	335	-	340	-
Mg	mg L^{-1}	21.1	<0.05	↓	<0.05	↓	<0.05	↓	<0.05	↓
Ca	mg L^{-1}	66.9	69.9	↑	61.2	↓	63.7	↓	75.6	↑
Mn	µg L^{-1}	180	3.39	↓	2.92	↓	3.16	↓	2.59	↓
Fe	mg L^{-1}	0.11	<0.03	↓	<0.03	↓	<0.03	↓	<0.03	↓
S	mg L^{-1}	41	29.9	↓	42.1	-	30	↓	41.8	-
Cl	mg L^{-1}	454	402	↓	422	↓	407	↓	427	↓
Ni	µg L^{-1}	0.14	0.08	↓	<0.05	↓	<0.05	↓	<0.05	↓
Al	µg L^{-1}	15.5	79.7	↑	93.3	↑	74.5	↑	81.1	↑
Cd	µg L^{-1}	<0.02	0.02	-	0.04	↑	<0.02	-	0.03	↑
Cr	µg L^{-1}	0.3	0.79	↑	0.59	↑	0.48	↑	0.6	↑
Zn	µg L^{-1}	6.8	13.1	↑	12.2	↑	13.1	↑	12.2	↑

The concentration of bacterial 16S rRNA gene copies analyzed by qPCR in the samples was used as a proxy for bacterial biomass. Compared to groundwater in the beginning of the experiment (2.6×10^5 copies mL^{-1}), the number of planktonic bacteria in the water was low in all carbon steel-containing mesocosms, 3.0×10^2 copies mL^{-1} in the biotic experiment (Figure 1). Interestingly, in water from the stainless steel-containing mesocosms the amount of planctonic bacteria was 10-fold higher, 1.8×10^3 copies mL^{-1} (Figure 1). The number of sulphate reducing microbes in the water in all mesocosms was low, below 80 copies mL^{-1} whereas in the beginning of the experiments 1.3×10^5 copies mL^{-1} was detected (Figure 1).

Biofilm formation on the surface of carbon steel was more intense than on the surface of stainless steel, showing 1.14×10^4 and 5.8×10^3 16S rRNA gene copies cm^{-1}, respectively (Figure 2). The amount of sulphate reducing microbes on the carbon steel surface was 2.1×10^2 copies mL^{-1} (Figure 2). On the surface of stainless steel the amoun of sulphate reducing microbes fell below detection limit of the assay. The number of methanogenic archaea in all samples was low and fell below the detection limit of assay.

The composition of the biofilm was studied in more detail by pyrosequencing of the bacterial 16S rRNA gene. In accordance to the qPCR analysis, the biofilm formation was greatest on the surface of carbon steel in the biotic treatment (Figure 2). The DNA extracted from carbon steel from the biotic mesocosm provided enough sequence reads for reliable phylogenetic analysis to be conducted, i.e. 861 sequence reads that passed quality control. The biofilm formed over one year on the stainless steel was too sparce for detection by the assay.

The majority of the biofilm-forming bacteria detected on the surface of the carbon steel belonged to phylum Proteobacteria (62%) (Figure 3). The second largest group belonged to phylum Firmicutes (16%) (Figure 3).

Of the Proteobacteria, different α-proteobacterial taxa contributed with the greatest part (Fig. 4). The largest OTU (OTU 1 containing 208 sequences) was most closely related to the *Methylobacterium jeotgali* and *Methylobacterium* extorquens. Both of these species are facultative methylotrophs that in addition to methanol are able to use C_2, C_3 and C_4 compounds for growth (Figure 4). The second largest OTU (OTU 2 containing 90 sequences) resembled *Afipia broomeae* and nitrogen-fixing *Bradyrhizobium diazoefficiens* (Figure 4).

Clostridia was the most abundant class of the Firmicutes. The majority of the clostridial OTUs most closely resembled *Desulfosporosinus youngiae* a spore forming sulfate-reducing bacteria (Figure 5).

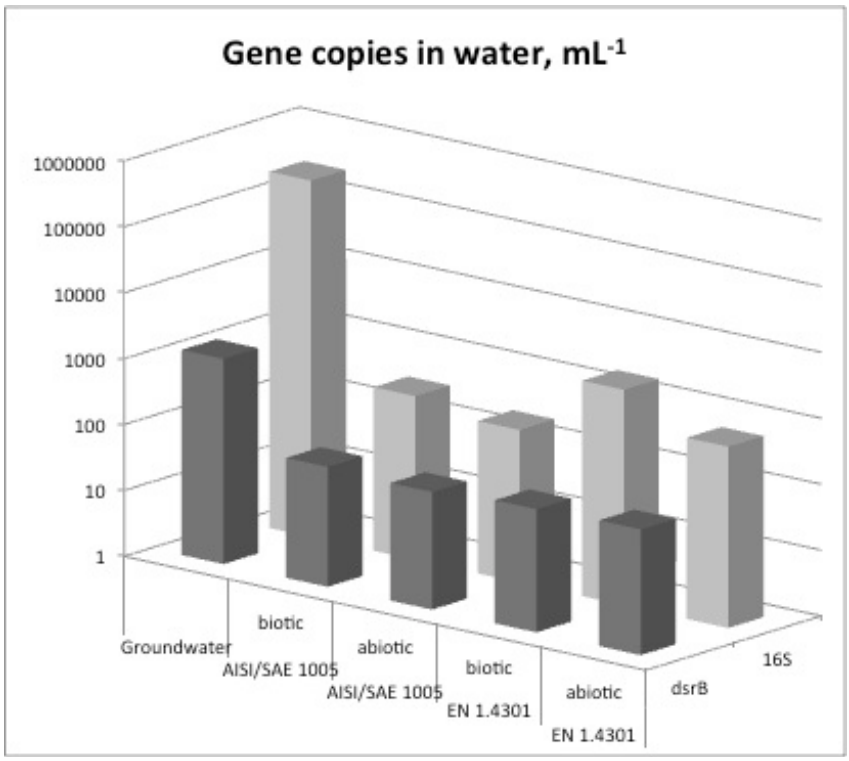

Fig. 1. 16S rRNA and *dsr*B gene copies detected freely from the water incubated with metals.

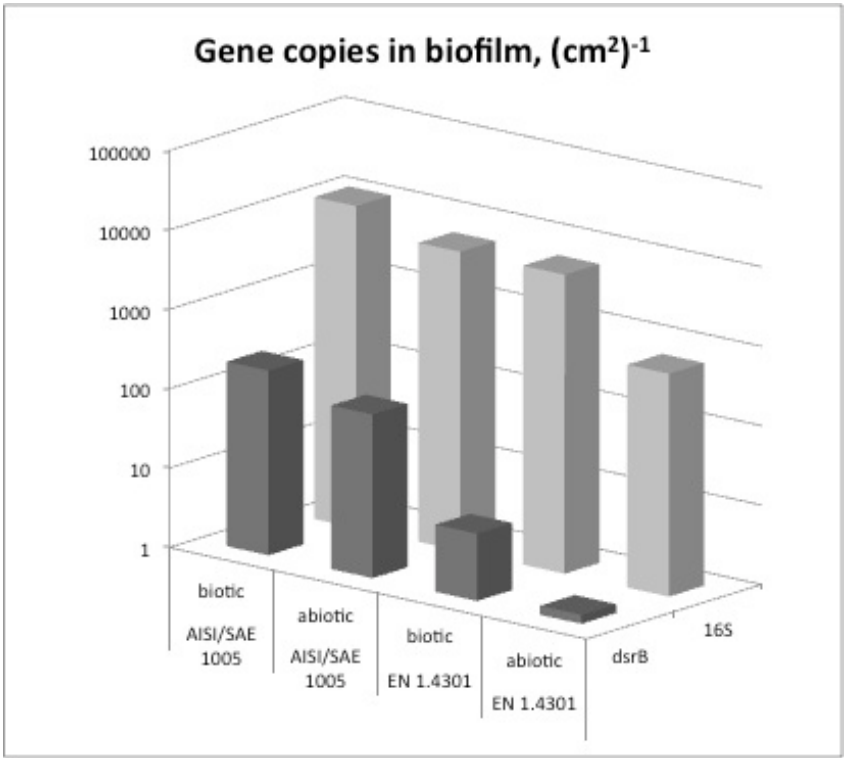

Fig. 2. 16S rRNA and *dsr*B gene copies detected from the biofilm formed on surface of metals.

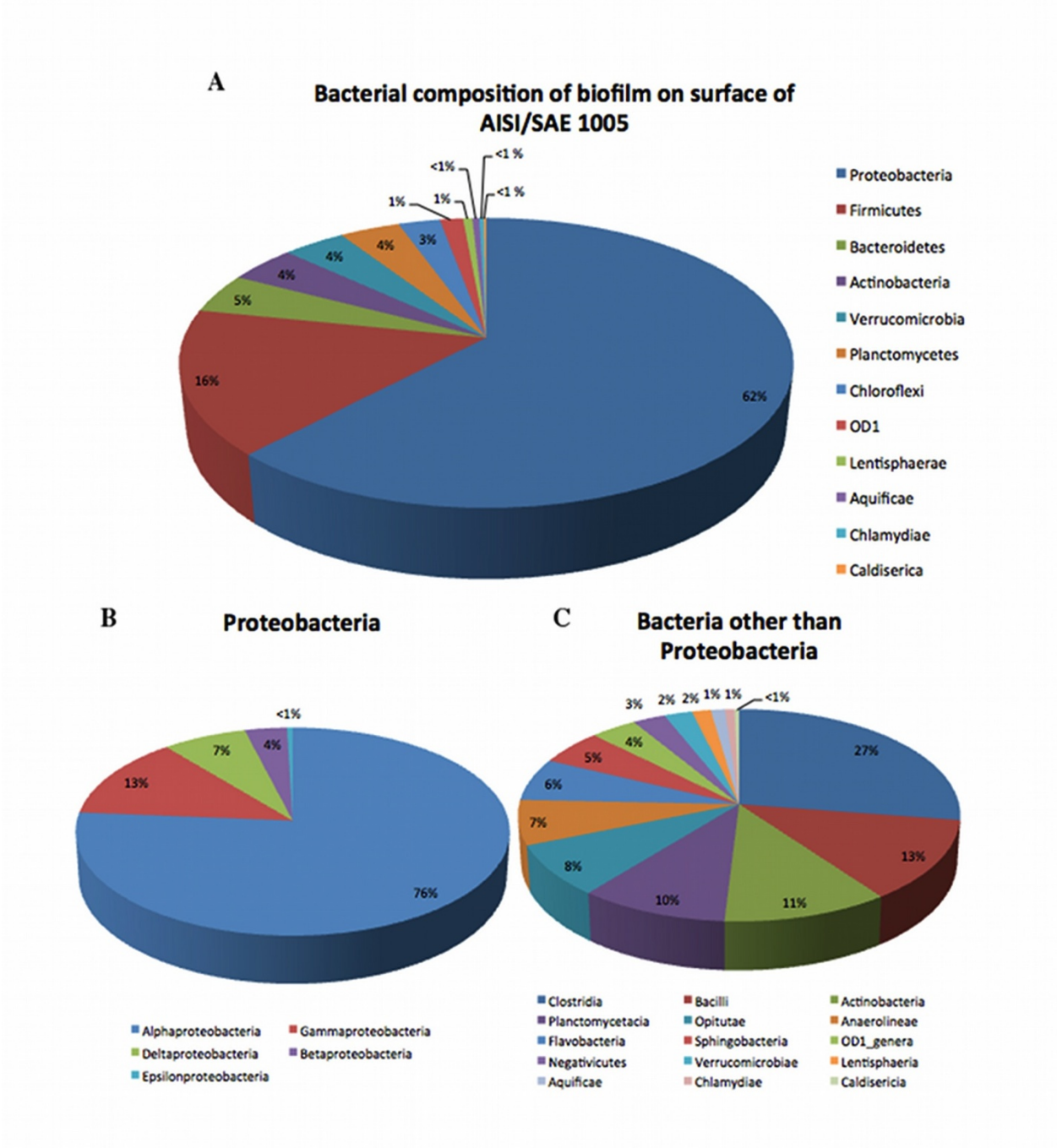

Fig. 3. A) The diversity and abundance of bacterial phyla detected on the surface of carbon steel AISI1005 after 12 months. All sequences of OTUs belonging to species within a phylum have been combined. B) The diversity and abundance of Proteobacteria. C) The diversity and abundance of bacteria other than Proteobacteria.

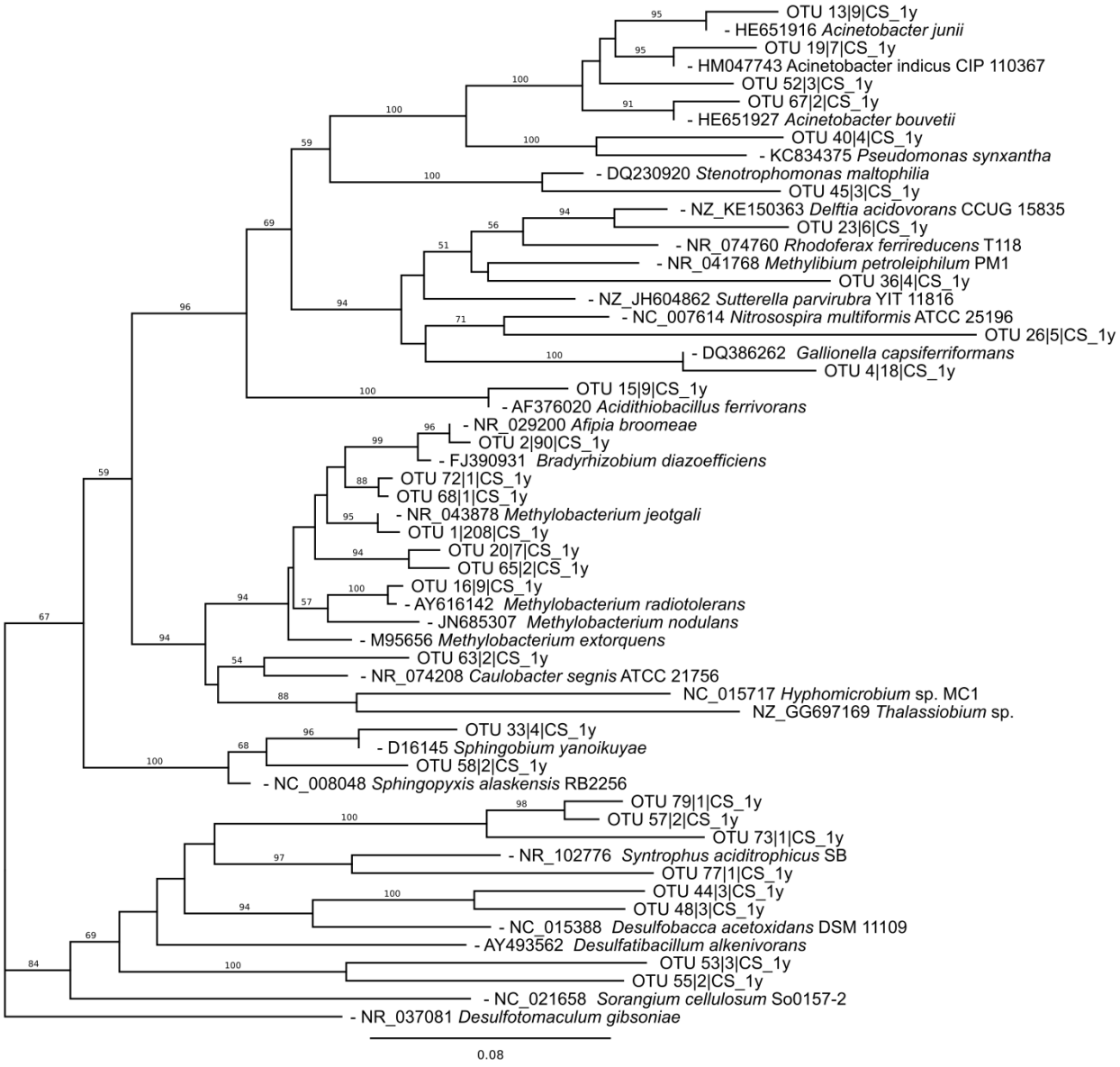

Fig. 4. Phylogenetic tree of proteobacterial diversity, based on the 16S rRNA gene sequences obtained by 16S rRNA gene-based pyrosequencing, in relation to relevant reference sequences and sequences of type species relatives. Bootstrap values, calculated from 1000 repetitions, are shown at branch points with > 50% support. The scale bar indicates 0.08 nucleic acid substitutions. The tree is rooted by *Desulfotomaculum gibsoniae.*

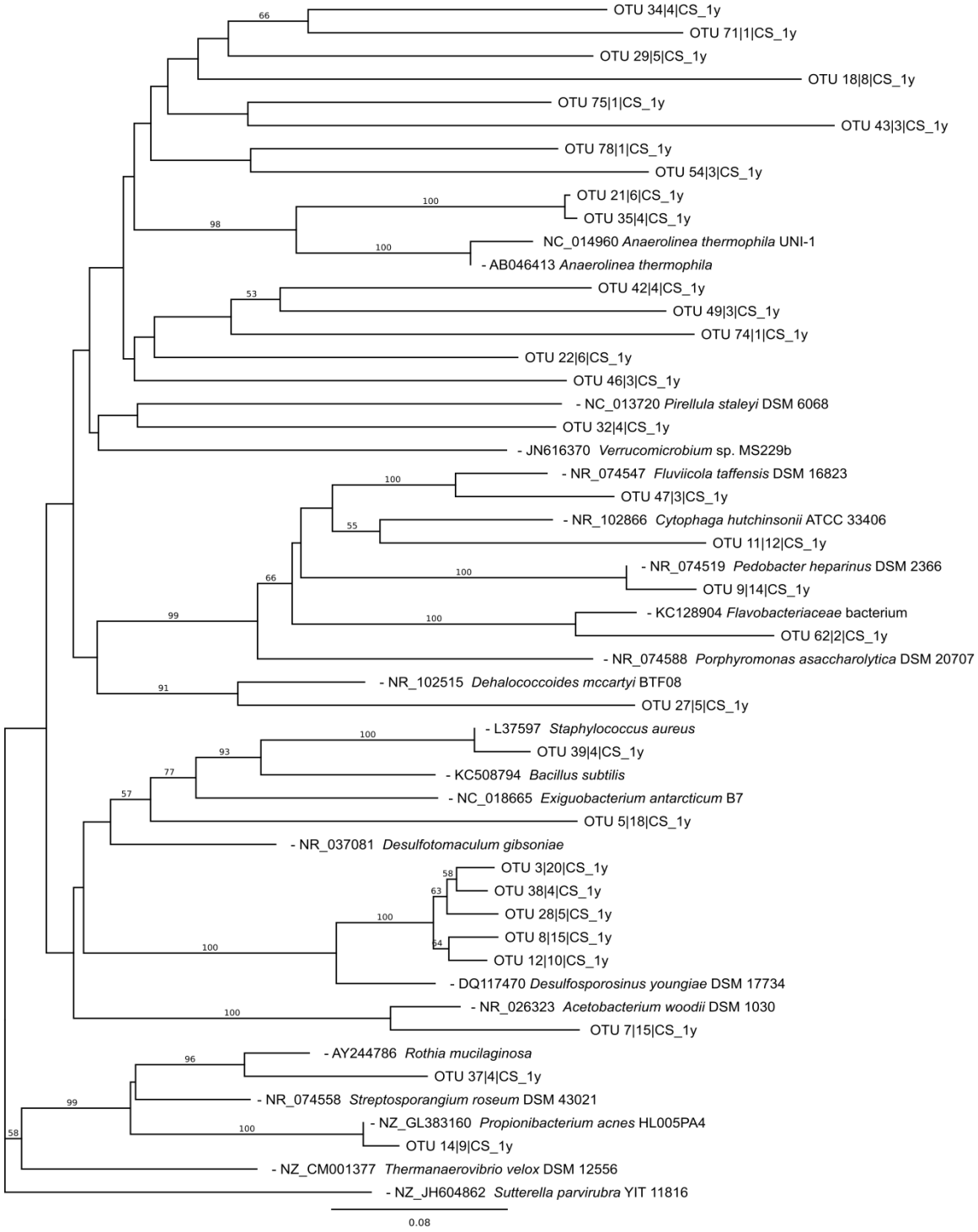

Fig. 5. Phylogenetic tree of bacterial diversity, excluding the proteobacteria, based on the 16S rRNA gene sequences obtained by 16S rRNA gene-based pyrosequencing, in relation to relevant reference sequences and sequences of type species relatives. Bootstrap values, calculated from 1000 repetitions, are shown at branch points with > 50% support. The scale bar indicates 0.08 nucleic acid substitutions. The tree is rooted by *Sutterella parvirubra.*

According to the weight loss measurements the corrosion rate of carbon steel in alkaline, low oxygen groundwater was very low (< 0.5 µm a^{-1}) both in the biotic as well as abiotic environment. The corrosion rate in the biotic environment varied from 0.11 to 0.16 µm a^{-1} whereas it was a little higher in the abiotic environment (0.27 to 0.35 µm a^{-1}). After the incubation the carbon steel coupons were covered with a yellowish deposit layer with some dark and red areas. Closest to the metal surface a dark layer could be seen. Visually in both biotic and in abiotic environments the formed layers were similar except that in the abiotic environment more red areas could be seen, under which mild corrosion was detected. This was confirmed under stereomicroscope observations after removing the deposit layers where more corrosion dots on the surface as well as some deeper localized corrosion pits at the edge or close to the edges of the coupons from the abiotic environment could be seen.

A thin yellowish deposit layer could be seen also on the surfaces of the stainless steel coupons. However, in this case, no corrosion was detected on the surfaces of the stainless steel after removing the deposit layer. In addition, no weight loss was observed and measurable corrosion rates could not be detected in the samples.

Closer examination by FE-SEM showed that the deposits on the surface of steel coupons differed greatly between the biotic and abiotic experiments, as well as between the carbon steel and stainless steel (Figures 6 and 7).

The light yellowish deposit on the surfaces of the carbon steel specimen was found to contain calcium and oxygen as main components in both the biotic and abiotic alkaline groundwater environments. High amounts of magnesium, silicon and iron could also be detected from these yellowish deposits in both cases. The amount of calcium was higher in abiotic coupon (34 w-% compared to 21 w-% in biotic coupon). Whereas the amount of magnesium and iron were a little lower (11 w-% and 14 w-% for Mg and 5 w-% and 9 w-% for Fe respectively). The red and dark areas on the surfaces contained iron and oxygen as main components and smaller amounts of magnesium, silicon and calcium. There were more iron and less oxygen, magnesium and silicon in these deposits on abiotic coupon compared to those on biotic coupon. Oxygen, calcium, iron, magnesium and silicon were the main components detected from the surfaces of the stainless steel specimens held in both environments. In addition to iron, also other stainless steel alloy compounds (chromium, nickel and manganese) could be detected in the EDS analyses from the surfaces of stainless steel specimens.

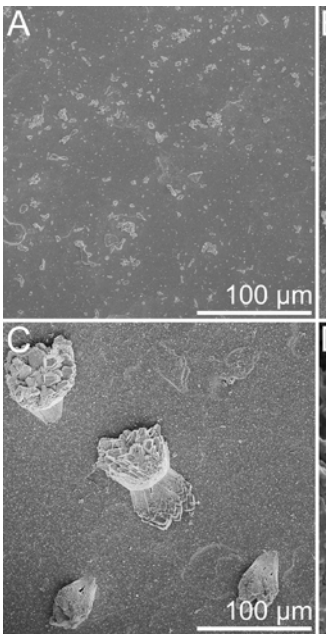

Fig 6. The surface of AISI/SAE 1005 detected with FE-SEM. A-B) Biotic environment, C-D) Abiotic environment.

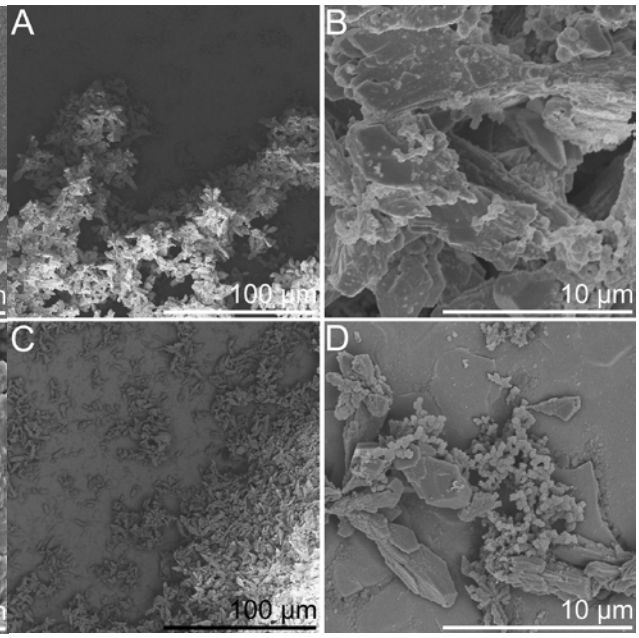

Fig 7. The surface of EN 1.4301 detected with FE-SEM. A-B) Biotic environment, C-D) Abiotic environment.

DISCUSSION

Alkalinity caused by concrete impeded greatly the microbial corrosion rate and inhibited the biofilm formation. High alkalinity is known to protect low alloy steels from corrosion, also other than microbially induced corrosion. The corrosion rates detected in this study were far from those observed earlier in the same groundwater conditions as in this study but without concrete; namely 10 to 63 µm a^{-1} [14]. In addition, a corrosion rate of 9.5 µm a^{-1} was detected on carbon steel after a12 months incubation in a laboratory scale study in a mesocosm containing groundwater from the same Olkiluoto site as in the present study and to which glucose had been added as carbon source for the microorganisms but no crushed concrete had been added [13].

The results from pyrosequencing and qPCR analysis indicated that the stainless steel surface did not provide as favorable conditions for biofilm formation as did the surface of carbon steel in alkaline groundwater environment. However, although the surface of the stainless steel appeared to be a less suitable surface for biofilm formation than the surface of carbon steel, the number of 16S rRNA genes detected from water incubated with stainless steel was an order of magnitude higher than that of the carbon steel-containing mesocosm.

The composition of the biofilm detected on carbon steel in this study was different from that detected previously from this waste disposal site [13]. In neutral pH as reported in [13], β-proteobacteria dominated in the biofilm formed on carbon steel, but when concrete raised the pH of the groundwater, α-proteobacteria became enriched and dominated in the biofilm. In this study, the biofilm predominantly consisted of α-proteobacterial methylotrophic bacteria belonging to *Methylobacterium* species. Methylotrophic bacteria are able to utilize simple one carbon compounds [15] as carbon substrates for growth. These types of carbon compounds are

common in deep groundwater, and in the bedrock aquifers of the Fennoscandian shield area the available carbon is often present as small carbon compounds. The alkaline environment also appears to benefit growth of the methylotrophic α-proteobacteria bacteria [16].

CONCLUSIONS

The results of this simulation study show that high alkalinity slows the onset of biofilm formation when compared to pH neutral conditions. The corrosion rate of carbon steel was low after the one-year period of exposure to disposal conditions. No corrosion was detected on the stainless steel at the end of the exposure period. It appears that in presence of concrete the microbially induced corrosion is slow, at least over a short time period.

However, the results obtained here and in previous studies show that the natural microorganisms inhabiting groundwater are able to form biofilm in different conditions. The microbial diversity in natural ground water is vast and they may be able to adapt changing environmental conditions.

REFERENCES

1. S. Haveman, K. Pedersen and P. Ruotsalainen, “Distribution and Metabolic Diversity of Microorganisms in Deep Igneous Rock Aquifers of Finland,” *Geomicrobiology Journal* **16**, 4 (1999).
2. G. Muyzer, E. de Waal and A. Uitierlinden, “Profiling of complex microbial populations by denaturing gradient gel electrophoresis analysis of polymerase chain reaction-amplified genes coding for 16S rRNA,” *Appl Environ Microbiol.* **59**: 695-700 (1993).
3. J. Geets *et al*., “*Dsr*B gene-based DGGE for community and diversity surveys of sulphate-reducing bacteria,” *J Microbiol Meth.* **66**: 194-205 (2006).
4. M. Wagner, A. Roger, J. Flax, G. Brusseau and D. Stahl, “Phylogeny of dissimilatory sulfite reductases supports an early origin of sulphate respiration,” *J Bacteriol.* **180**: 2975-2982 (1998).
5. Hales B, *et al*., “Isolation and identification of methanogen-specific DNA from blanket bog peat by PCR amplification and sequence analysis,” *Appl Environ Microbiol.* **62**: 668-675 (1996).
6. U. Edwards, T. Rogall, H. Blöcker, M. Emde and E. Böttger, “Isolation and direct complete nucleotide determination of entire genes. Characterization of a gene coding for 16S ribosomal RNA,” *Nucleic Acids Res* **17**: 7843-53 (1989).
7. M. Bomberg, M. Nyyssönen and M. Itävaara, “Characterization of Olkiluoto bacterial and archaeal communities by 454 pyrosequencing,” Posiva Working Report **31** (2011).
8. P. Schloss, *et al*., “Introducing mothur: Open-source, platform-independent, community-supported software for describing and comparing microbial communities,” *Appl Environ Microbiol* **75**: 7537-41 (2009).
9. AJ. Drummond *et al*., Geneious v5.3, (2010). Available from http://www.geneious.com
10. S. Guindon S and O. Gascuel , “A Simple, fast, and accurate algorithm to estimate large phylogenies by maximum likelihood,” *Syst Biol.* **52**: 696-704 (2003).
11. TH. Jukes and CR. Cantor, *Evolution of Protein Molecules*. pp. 21–132. New York: Academic Press (1969).
12. ASTM G 1-90 (Reapproved 1999), “Standard Practice for Preparing, Cleaning, and Evaluating Corrosion Test Specimens” (West Conshohocken, PA: ASTM). (1999)

13. L. Carpén, P. Rajala, M. Vepsäläinen and M. Bomberg, “Corrosion behaviour and biofilm formation on carbon steel and stainless steel in simulated repository environment” Eurocorr2013, paper no. 1589. (2013).
14. L. Carpén, J. Maukonen and S. Salo, “Accelerated corrosion of carbon steel and zinc in oxygen-free groundwater - Due to the microbiological activity?,” Nace International Corrosion Conference & Expo 2012, March 11-15, 2012, Salt Lake City, Utah, USA. Nace International, ss. C2012-0001397 (2012).
15. R. Hanson and T. Hanson, “Methanotrophic bacteria,” *Microbiol Rev* **60**: 439-71 (1996).
16. R. Kietäväinen, *et al*., “Characterisation and isotopic evolution of saline waters of the Outokumpu Deep Drill Hole, Finland – Implications for water origin and deep terrestrial biosphere,” *Appl Geochem*. **32**: 37-51 (2013).

ACKNOWLEDGEMENTS

This work was funded by the KYT2014, Finnish Research Program on Nuclear Waste management (REMIC-project). The help of the staff in TVO Oyj Olkiluoto Nuclear Power Plant during the samplings is gratefully acknowledged. The authors thank the skilful assistance of Mirva Pyrhönen, Taru Lehtikuusi and Seppo Peltonen in the experimental work.